Role of Fine Clays in Bitumen Extraction from Oil Sands

Jianjun Liu, Zhenghe Xu, and Jacob Masliyah
Dept. of Chemical and Materials Engineering, University of Alberta, Edmonton, AB T6G 2G6, Canada

DOI 10.1002/aic.10174
Published online in Wiley InterScience (www.interscience.wiley.com).

Clay minerals such as montmorillonite and kaolinite are considered as fine solids that could adversely affect bitumen extraction from oil sands. Colloidal forces between bitumen and fine clays and between bitumen and bitumen in the presence of montmorillonite clays were measured with an atomic force microscope. Although long-range repulsive forces between bitumen and kaolinite or montmorillonite were similar, stronger adhesion forces were measured between bitumen and montmorillonite than between bitumen and kaolinite, in particular when calcium ions were present. The presence of montmorillonite clays with calcium addition diminished the adhesive forces between bitumen surfaces. Zeta potential distributions of bitumen droplets and clays, individually or in a mixture, were measured in the presence of 1 mM calcium ions. The results showed that kaolinite clays deposited weakly on the bitumen surface, whereas montmorillonite clays attached strongly to bitumen. Such strong montmorillonite clay attachment set a barrier for bitumen droplets to coagulate with each other and to attach to air bubbles. This behavior accounts for the observed detrimental synergetic effect of montmorillonite clays and calcium ions on bitumen recovery by flotation. © 2004 American Institute of Chemical Engineers *AIChE J,* 50: 1917–1927, 2004
Keywords: bitumen, colloidal force, adhesive force, montmorillonite clay, kaolinite clay, AFM, oil sands

Introduction

Bitumen extraction from oil sand ores in Alberta represents a mega-scale operation, mining and processing more than 1000 tons ore/min to produce an oil supply for more than 30% overall Canadian oil demand. The Athabasca oil sand deposits in Alberta typically contain 6–14 wt % bitumen and 80–85 wt % mineral solids (mainly quartz and clays such as kaolinite, illite, and some montmorillonite), balanced by water. A water-based extraction process (Helper and Hsi, 1989; Helper and Smith, 1994) includes two essential micro-subprocesses: bitumen "liberation" and "aeration." Together, these two micro-subprocesses determine bitumen recovery. "Liberation," defined as the detachment of bitumen from sand grains, is prerequisite for bitumen extraction. The "aeration" is a process where liberated bitumen droplets attach to air bubbles to achieve effective flotation. In this case, the hydrophobicity of the bitumen surface and the size of bitumen droplets are critical.

The hydrophobicity of the bitumen surface and the size of bitumen droplets are related to the physicochemical conditions of bitumen extraction systems, such as slurry pH and the content of metal ions and fines in the mined ore and in the recycled process water. As an example, for a "good processing" ore containing about 10% bitumen and low fines content ($\lesssim$10% of total minerals), a high bitumen flotation rate (high bitumen recovery and good froth quality) can be obtained with the water-based extraction technology. However, for "poor processing" ores, which contain about 8% bitumen and a substantially larger amount of solid fines (up to $\sim$35% of total minerals), the current water-based extraction process generates a high percentage of small ($<$100 microns) bitumen droplets

Correspondence concerning this article should be addressed to Z. Xu and J. Masliyah at zhengehe.xu@ualberta.ca and jacob.masliyah@ualberta.ca, respectively.

and suffers from either low bitumen recovery or poor froth quality in both industrial operations and in laboratory tests (Sanford et al., 1979, 1983; Smith and Schramm, 1992; Takamura and Wallace, 1988; Zhou et al., 1999). In general, bitumen recovery was observed to decrease with increasing fines content in the oil sand ores and metal ion concentration in the process water (Helper and Hsi, 1989; Helper and Smith, 1994). The presence of excessive amount of fines in the "poor processing" ore coupled with high divalent ion concentration in the process water is one of the main reasons for its poor processability. Here fines are defined by oil sands industry as the percentage of solids smaller than 44 microns. Test results have shown a high correlation between ore processability and content of fines having a size smaller than 2 microns. Slime coating, defined as a layer of fine gangue particles coating on valuable minerals (Fuerstenau, 1980; Sivamohan, 1990) and controlled by colloidal forces, is recognized to have a profound impact on the micro-subprocesses in flotation and hence on bitumen extraction from oil sand ores. The presence of slime coating not only reduces the bitumen flotation rate and recovery by setting up a steric barrier retarding bitumen droplets to contact with air bubbles, but also deteriorates the froth quality by carrying fine materials attached to the bitumen to the froth product, which bears significant implications for subsequent froth treatment.

To understand the impact of fines on the bitumen extraction, a systematic research program was initiated in our research group. Batch flotation (Kasongo et al., 2000) test results showed a sharp depression of bitumen recovery only when montmorillonite clays, at about 1 wt % of oil sands ore, were added together with greater than 30 ppm calcium ions to oil sands processing pulp, hereby suggesting a detrimental synergetic effect of calcium ions with montmorillonite clay. Such a depression was not observed with the combination of calcium ions and kaolinite or illite, and with individual addition of calcium or clays. The possible coating of montmorillonite clays on bitumen surfaces in the presence of 1 mM Ca (~40 ppm) was also evaluated in our laboratory by examining bitumen–bubble attachment using impinging jet cells (Yang et al., 2000a,b). It was found that only the combination of montmorillonite clays and calcium ions decreased significantly the flux of gas bubbles attaching to the bitumen surface. In contrast, the presence of clays or calcium alone, or the combination of calcium with kaolinite showed little effect on the gas bubble flux attaching to the bitumen surface. The induction time measurement (Gu et al., 2003) led to a similar conclusion for bitumen and air bubble attachment in the presence of montmorillonite and calcium. Recently, zeta potential distribution measurement was used to examine qualitatively the interactions between bitumen and clays (Liu et al., 2002a). Montmorillonite clays were found to strongly attach to a bitumen surface in the presence of 1 mM (~40 ppm) calcium ions. It can be hypothesized that a layer of montmorillonite clay particles coats the bitumen surface in the presence of calcium ions. This layer of hydrophilic or much less hydrophobic montmorillonite clay particles on bitumen droplets act as a barrier for bitumen–bitumen coagulation and bitumen–air bubble attachment, thereby leading to a low attachment efficiency and hence low bitumen flotation rate.

In this study, surface forces between bitumen and montmorillonite or kaolinite clays were measured with an atomic force microscope to understand the slime coating phenomenon. To further study the role of fines in bitumen extraction, the interaction forces between bitumen and bitumen in the presence of montmorillonite clay particles in aqueous solutions were also measured. The measured force profiles are used to qualitatively interpret the role of fine clays in bitumen extraction from oil sand ores. The obtained results were further confirmed by the zeta potential distribution measurements.

Experimental

Materials

In this study, extracted bitumen from froth treatment was provided by Syncrude Canada Ltd. Silica microspheres (~8 μm) purchased from Duke Scientific (Palo Alto, CA) were used for preparation of probing bitumen surface. Two types of clays, kaolinite and montmorillonite, were purchased from Ward's Natural Science (Rochester, NY) and used without further purification. Pseudo-spherical clay particles (agglomerates) about 5–10 μm were selected under an optical microscope for colloidal force measurements. The individual particles were characterized by X-ray microanalysis with an energy dispersive X-ray analyzer (EDX) in a scanning electron microscope (SEM) after force measurements. For zeta potential measurements, the clay sample was manually ground in a mortar to about 2–4 μm. Silicon wafers of 1-0-0 crystal planes were purchased from MEMC Electronic Materials (Merano, Italy) and used as the substrate for preparation of bitumen surfaces by spin-coating method. Reagent-grade HCl and NaOH (Fisher Scientific, Pittsburgh, PA) were used as pH modifiers. Ultrahigh purity KCl (>99.999%, Aldrich, Milwaukee, WI) was used as the supporting electrolyte, whereas reagent-grade $CaCl_2$ (99.9965%, Fisher) was used as the source of calcium ions. Reagent-grade toluene (Fisher) and home-distilled absolute ethanol were used as the dilution and cleaning solvents, respectively. The deionized water with a resistivity of 18.2 MΩ·cm, prepared with an Elix 5 followed by a Millipore-UV plus ultra water purification system, was used throughout this study.

Probe particle and bitumen surface preparation

Silica spheres or clay particles were glued with a two-component epoxy (EP2LV, Master Bound, Hackensack, NJ) onto the tip of a short wide-beam AFM cantilevers. The spring constant of the cantilever was calculated from its geometry determined from scanning electron micrographs (Veeramasuneni et al., 1996). The glued probe particles were allowed to set in a vacuum desiccator for more than 24 h. The particles were then exposed to an ultraviolet light for more than 5 h to remove any possible organic contaminants. The bitumen substrate surface was prepared with a P6700 spincoater (Specialty Coating Systems, Indianapolis, IN), whereas the bitumen probe surface was prepared with a dip-coating technique, described elsewhere (Liu, 2004). The early study has shown that bitumen films prepared with the two methods are suitable for colloidal force measurements, and the bitumen deformation during the force measurement is negligible for accurate data analysis.

The exact size of the probe particles used in each set of experiments was determined with SEM after the force measurement. Figure 1 shows typical SEM micrographs of pre-

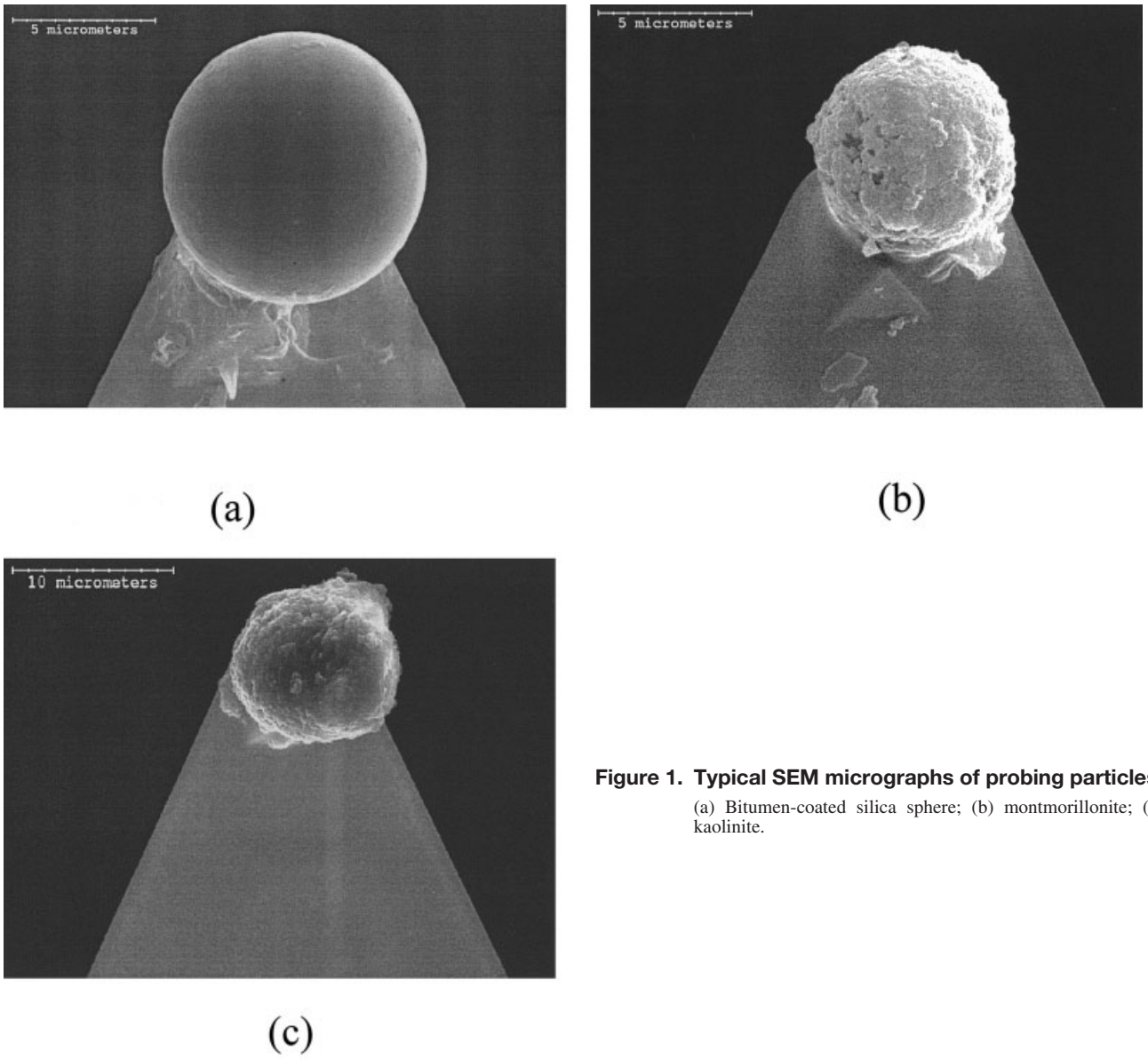

Figure 1. Typical SEM micrographs of probing particles.

(a) Bitumen-coated silica sphere; (b) montmorillonite; (c) kaolinite.

pared (a) bitumen-coated silica, (b) montmorillonite, and (c) kaolinite probing particles on the AFM cantilever.

Surface force measurement (AFM technique)

Surface force measurement was carried out with a Nanoscope® E AFM (Digital Instrument, Santa Barbara, CA). It consists of a piezoelectric translation stage, a cantilever substrate, a laser beam system, a split photodiode, and a fluid cell. The spin-coated bitumen substrate was glued onto a magnetic plate that was mounted on the piezoelectric translation stage. The cantilever substrate with a probe particle was mounted in the fluid cell. The solution was injected into the fluid cell slowly and the system was allowed to stabilize for 1 h before measurements. When the piezo stage brings the bitumen substrate to approach or depart from the probe particle in the vertical direction, the force between the two surfaces causes the cantilever spring to deflect upward or downward, depending on the force between them. The deflection of the cantilever spring was detected by the position-sensitive laser beam that is focused on the upper surface of the spring cantilever, and reflected to the split photodiode through a mirror. From the displacement of the piezo stage and the deflection of the spring cantilever, the long-range force between the substrate and the probe particle can be obtained. Adhesive force (pull-off force) data were collected under loading forces of 8–10 mN/m (the loading force was defined as the maximum force in the "constant compliance region"). It was found that the adhesive forces are independent on the loading forces in the range examined. Details related to the principles for colloidal force measurement using AFM can be found in the literature (Ducker et al., 1992; Kappl and Butt, 2002; Rabinovich et al., 1994). For quantitative comparison and theoretical analysis, both the measured interaction forces and adhesive forces were normalized with the mean radius R of the probe sphere. For the less well defined clay particles, the measurement was repeated with at least eight bitumen–clay pairs and plotted together to show a

Table 1. Hamaker Constants: B for Bitumen, C for Clay, and W for Water

Material	Bitumen	Water	Clay	B–W–B	B–W–C
Hamaker constant, A (10^{-20} J)	6 (Vincent, 1973)	3.7 (Israelachvili, 1991)	10 (Israelachvili, 1991)	0.28	0.65

general trend. All the experiments were conducted at room temperature of 22 ± 0.1°C.

To further confirm the interactions between bitumen and montmorillonite clay, the force measurements were carried out between bitumen surfaces conditioned with montmorillonite clay suspensions. Montmorillonite clay suspension was prepared by dispersing ground montmorillonite clays in water at a solid concentration of 0.1 wt % under ultrasonication for 10 min, followed by settling for 6 h to remove any coarse particles. The supernatant was used as a montmorillonite clay conditioning suspension for force measurements. During the force measurement, the supernatant was first injected into the fluid cell to contact bitumen surfaces for about 0.5 h, and then replaced with a clear solution containing the same electrolyte levels to avoid any disturbance from the suspended solids in the medium during the force measurement.

The measured long - range forces were fitted with the classical DLVO (Derjaguin–Landau–Verwey–Overbeek) theory. From the reported Hamaker constant value of mica (10×10^{-20} J) for montmorillonite and kaolinite (Isrealachvili, 1991) and 6×10^{-20} J for bitumen (Vincent, 1973), the combined Hamaker constants for bitumen/water/bitumen (A_{BWB}) and bitumen/water/montmorillonite or kaolinite clay (A_{BWC}) system were calculated to be 2.8×10^{-21} and 6.5×10^{-21} J, respectively, as shown in Table 1. The electrostatic double-layer forces between two surfaces were calculated numerically by solving the nonlinear Poisson–Boltzmann equation and force balance equation. The bitumen surface is assumed to be of constant surface charge density, given that its surface charge arises mainly from irreversible adsorption of surfactants. The clay surface is of constant surface potential because its surface charge arises primarily from adsorbing ions from solution (Hunter, 1993; Liu, 2004; Warszynski et al., 1997). It should be noted that, in reality, the assumption of constant surface charge density and constant surface potential constitutes the upper and lower limits of interaction forces, respectively. During the fitting exercise, Stern potentials [the potential at the Stern plane in the Stern–Grahame electric double-layer model (Masliyah, 1994)] for both surfaces as well as the decay length (κ^{-1}) were set as adjustable parameters. The measured zeta potential [the potential at the shear plane in the Stern–Grahame electric double-layer model (Masliyah, 1994)] values and calculated decay length from electrolytes used in the probing medium are used as a guide to set the initial values for Stern potentials and the decay length (κ^{-1}), respectively. A Visual Basic program running on EXCEL spreadsheet was developed in our laboratory for a general DLVO theory of asymmetrical surfaces in symmetrical/asymmetrical electrolyte solutions (Liu, 2004). The program was checked with known systems. When the fitting with the classical DLVO theory was found to be extremely poor, the DLVO theory was extended by including a hydrophobic force. The normalized hydrophobic forces can be expressed with a power law (Rabinovich and Yoon, 1994).

$$\frac{F_{HB}}{R} = -\frac{K}{6D^2} \tag{1}$$

where D is the separation of two surfaces, R is the radius of the probe sphere, and K is a constant for the hydrophobic force. The magnitude of K value depends on the surface hydrophobicity.

Zeta potential measurement

Zeta potential distributions of emulsified bitumen droplets and clay suspensions were measured with a Zetaphoremeter III (SEPHY/CAD). The detailed experimental procedures and principles have been described elsewhere (Liu et al., 2002a,b,c; Xu et al., 2003). The average of four independent measurements was reported in this communication.

Results and Discussion

Surface properties of clay mineral

Clay mineral is a layer-structured mineral (Olphen, 1976). The basic building elements are two-dimensional arrays of silicon–oxygen tetrahedral (T) and two-dimensional arrays of aluminum– or magnesium–oxygen–hydroxyl octahedral (O).

Montmorillonite clay is an expanding 2:1 (TOT) layer structured clay mineral. In the tetrahedral sheet, tetravalent Si is partly replaced by trivalent Al. In the octahedral sheet, the trivalent Al may be replaced by divalent Mg, Fe, Zn, and other atoms (designated isomorphous substitution), resulting in an excess of negative charge. This excess of negative charge is compensated by the adsorption on the layer surface of cations that are too large to be accommodated in the interior of the crystal. Therefore, the compensating cations on the layer surface can be easily exchanged with other cations when available in solution. With this special platy structure, montmorillonite clays feature some unique properties, such as high specific surface area, interlayer swelling, and large adsorption capacity of ions from a solution. Kaolinite, on the other hand, is a nonexpanding 1:1 (T:O) layer structured clay mineral. Because there is only a very small degree of isomorphous substitution and all the charge-compensating cations must adsorb on the

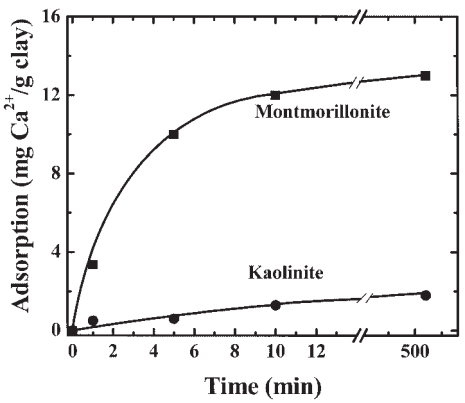

Figure 2. Calcium adsorption on clay minerals as a function of time in solutions containing initially 1 mM Ca^{2+} at a solid to liquid ratio of 1 g/L.

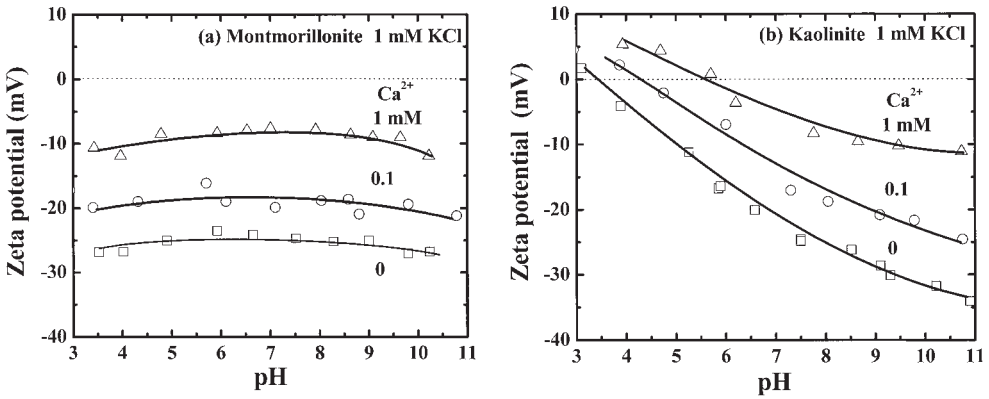

Figure 3. Average zeta potentials of clays as a function of pH.

Squares: in 1 mM KCl solutions; circles: in 1 mM KCl solutions containing 0.1 mM Ca^{2+}; up triangles: in 1 mM KCl solutions containing 1 mM Ca^{2+}. (a) montmorillonite; (b) kaolinite.

exterior surface of the stacked layer, kaolinite does not leave room for interlayer cations. Therefore, kaolinite shows minimal swelling in water, and the cation exchange capacity is relatively low.

Clearly, montmorillonite and kaolinite clays have different surface properties. As shown in Figure 2, montmorillonite clay exhibits a large capacity for ion adsorption from a solution, compared to that of kaolinite. Adsorption tests were conducted where montmorillonite or kaolinite clay at 1 g/L (clay/solution) was added to a 1 mM calcium solution. After conditioning for a given time, the suspension was filtered to remove the solids. The supernatant was then analyzed by use of the AA (atomic adsorption) technique. The results showed that 1 g of montmorillonite clay can adsorb up to 10.5 mg calcium in 5 min from a 1 mM calcium solution, whereas 1 g of kaolinite clay with a similar average particle size as montmorillonite clay can adsorb only 1.6 mg calcium in 500 min.

Similarly, there are some differences in zeta potentials of kaolinite and montmorillonite clays. The zeta potential of a montmorillonite clay suspension did not show a noticeable change with pH over the pH range from 3 to 11, as shown in Figure 3a. All the zeta potential values of montmorillonite clay particles are about -25 mV in a 1 mM KCl solution. Similar results were reported elsewhere by other researchers (Duran et al., 2000; Heath and Tadros, 1983; Sondi et al., 1996, 1997). This peculiar pH-independent behavior originates from the special platy structure of montmorillonite clays. Based on the structure of montmorillonite clays, the basal plane was considered to be of constant surface charge. In this case, H^+ and OH^- ions are not considered as potential-determining ions. Because only about 1% of the total surface area is from the amphoteric edges, the pH-independent zeta potential behavior of montmorillonite clays is not unexpected (Sondi et al., 1996, 1997). In the presence of calcium ions, the surface remains negatively charged over the pH range studied, although the magnitude of zeta potentials becomes smaller with calcium ion addition. This observation appears to be contradictory to the large uptake of calcium ions, as was shown in Figure 2. In contrast to the specific adsorption mechanism of calcium on a mineral surface, calcium ions adsorb on montmorillonite clay by a cation-exchange mechanism, which has less influence on the net surface charge. From the results in Figure 2, the residual Ca^{2+} concentration in the solution containing montmorillonite clays is 0.67 mM. The reduction in the magnitude of zeta potential of montmorillonite clays with calcium ion addition is attributed mainly to the compression of the electric double layer. As

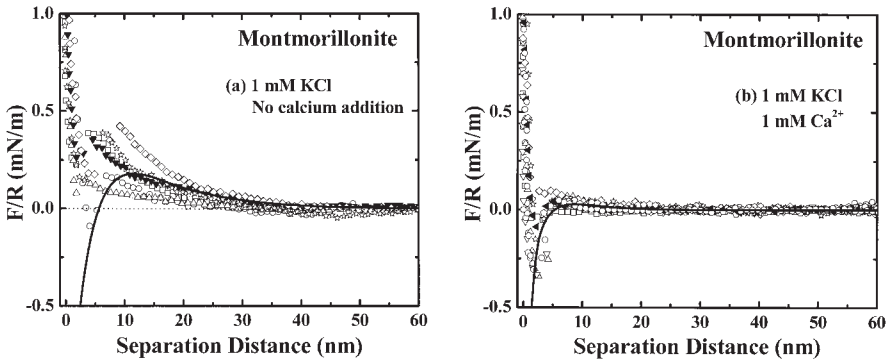

Figure 4. Normalized interaction forces (*F*/*R*) between bitumen and montmorillonite as a function of separation distance at pH 8.2.

Solid lines represent the classical DLVO fitting using $A_{BWC} = 6.5 \times 10^{-21}$ J with the best-fitted decay length and Stern potential being: (a) in 1 mM KCl solutions, $\kappa^{-1} = 9.4$ nm, $\psi_B = -70$ mV, $\psi_M = -18$ mV; (b) in 1 mM KCl solutions containing 1 mM Ca^{2+}, $\kappa^{-1} = 4.8$ nm, $\psi_B = -30$ mV, $\psi_M = -6$ mV.

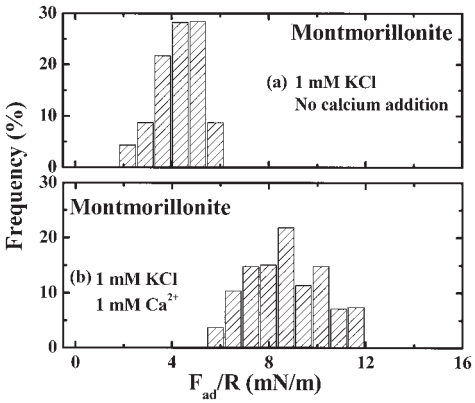

Figure 5. Distribution of normalized adhesive forces (F_{ad}/R) between bitumen and montmorillonite measured at pH 8.2 under loading forces of 8–10 mN/m.

(a): in 1 mM KCl solutions; (b): in 1 mM KCl solutions containing 1 mM Ca^{2+}.

shown in Figure 3b, the zeta potential values of kaolinite decreased with increasing suspension pH, with an iso-electric point (iep) at pH 3.6. The addition of calcium ions substantially depressed the zeta potential values. A noticeable shift in the iep from a pH of 3.6 to 5.7 with the addition of 1 mM calcium was observed, indicating some degree of specific adsorption of calcium ions on the kaolinite clay surfaces.

Bitumen–montmorillonite clay interaction

The measured force profiles for a number of bitumen–montmorillonite clay pairs are shown in Figure 4. In 1 mM KCl solutions at pH 8.2 without calcium addition (Figure 4a), the interaction force was highly repulsive, setting up a barrier for montmorillonite clay to approach the bitumen surface. The presented data are for a number of different clay particles. As would be anticipated, the data are highly scattered. This is explained by the surface roughness of the clay particles, as was shown in Figure 1b. However, the trend is very clear for the variation of the force vs. separation distance. To this end, the general conclusion derived from the data is valid and will be further illustrated using different conditions. The average force profiles at separation distance of greater than 8 nm can be fitted with the classical DLVO theory, as shown by the solid line in Figure 4a. This indicates that the electrostatic double-layer repulsive force dominates the long-range force profile.

In 1 mM KCl solutions containing 1 mM calcium ions at pH 8.2 (Figure 4b), the long-range repulsive forces were significantly depressed. The substantially decreased force barrier suggests that a montmorillonite clay particle can easily approach a bitumen surface. Again, the average force profile at a separation distance of greater than 6 nm can be reasonably fitted with the classical DLVO theory.

The normalized adhesion force distribution for a number of bitumen–montmorillonite clay pairs is shown in Figure 5. In 1 mM KCl solution at pH 8.2 in the absence of calcium (Figure 5a), the adhesion forces were centered at 4 mN/m. However, in the presence of 1 mM calcium ions (Figure 5b), the adhesion forces increased up to about 9 mN/m. The observed increase could be attributed to the fact that calcium ions strongly adsorbed on both montmorillonite clay (Figure 2) and bitumen surfaces (Liu et al., 2002a). This dual adsorption leads to bridging between bitumen and montmorillonite clay particles. The results clearly indicate that calcium addition can depress the repulsive force barriers and enhance the adhesion forces between bitumen and montmorillonite clay particles, thereby facilitating slime coating of montmorillonite clay particles on the bitumen surface.

Bitumen–kaolinite clay interaction

For bitumen and kaolinite clay, repulsive forces were observed in 1 mM KCl solutions at pH 8.2 without calcium addition, as shown in Figure 6a. The force profiles at a separation distance of greater than 8 nm can be reasonably described with the classical DLVO theory (the solid line in Figure 6a). By adding 1 mM calcium ions, the repulsive forces were depressed to zero, as shown in Figure 6b. From the consideration of long-range colloidal forces, one would expect a kaolinite clay particle to coat the bitumen in the presence of calcium, as was in the case of montmorillonite clay. However,

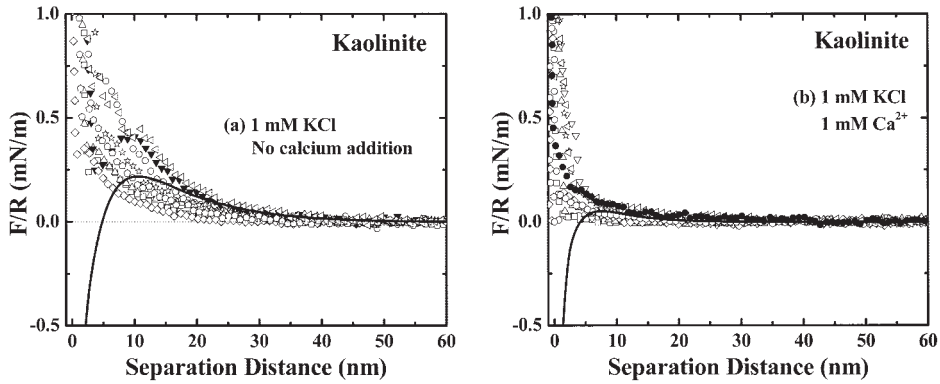

Figure 6. Normalized interaction forces (F/R) between bitumen and kaolinite as a function of separation distance at pH 8.2.

Solid lines represent the classical DLVO fitting using $A_{BWC} = 6.5 \times 10^{-21}$ J with the best-fitted decay length and Stern potential being: (a) in 1 mM KCl solutions, $\kappa^{-1} = 9.4$ nm, $\psi_B = -70$ mV, $\psi_K = -20$ mV; (b) in 1 mM KCl solutions containing 1 mM Ca^{2+}, $\kappa^{-1} = 4.8$ nm, $\psi_B =$ -32 mV, $\psi_K = -8$ mV.

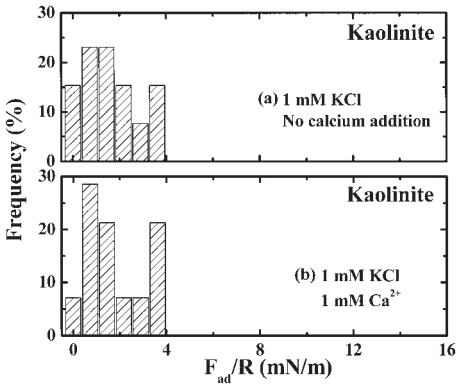

Figure 7. Distribution of normalized adhesive forces (F_{ad}/R) between bitumen and kaolinite measured at pH 8.2 under loading forces of 8–10 mN/m.

(a): in 1 mM KCl solutions; (b): in 1 mM KCl solutions containing 1 mM Ca^{2+}.

compared with montmorillonite clays, only a marginal slime coating was observed (Gu et al., 2003; Kasongo et al., 2000; Liu et al., 2002a; Yang et al., 2000a,b). To reconcile this apparent conflict, the adhesion forces have to be considered. As shown in Figure 7, the adhesive forces for bitumen–kaolinite pairs range from 0 to 4mN/m, which are lower than those for the pairs of bitumen and montmorillonite. Importantly, calcium addition did not enhance the adhesion forces between the bitumen and kaolinite clay particles. This is probably attributable to the weaker adsorption of calcium ions on the kaolinite clay surface. The present results indicate that kaolinite clay can only weakly attach to the bitumen surface even with calcium ion addition.

Bitumen–bitumen interaction

To further understand the role of montmorillonite clay addition in bitumen flotation, surface force measurements were carried out between bitumen surfaces conditioned with montmorillonite suspension in the absence and presence of calcium ions.

Absence of Clay. For comparison, the interaction force was measured at pH 8.2 for bitumen–bitumen in the absence of clays. As shown in Figure 8, the forces are repulsive with a jump-in at a separation of 4–5 nm. The addition of calcium ion dramatically depressed the long-range repulsive forces. This depression can be accounted for by the compression of the electric double layer. The force profiles at greater separation can be reasonably fitted with the classical DLVO theory, as shown by a dashed line in Figure 8. However, at shorter separation, a noticeable deviation of force profiles from the classical DLVO theory was observed. For example, this separation distance is about 12 nm for the case of no calcium, as shown by the dashed line in Figure 8. The force profiles over a separation range less than about 12 nm cannot be described unless the extended DLVO theory by including a hydrophobic force was used, as shown by solid lines in Figure 8. Measure-

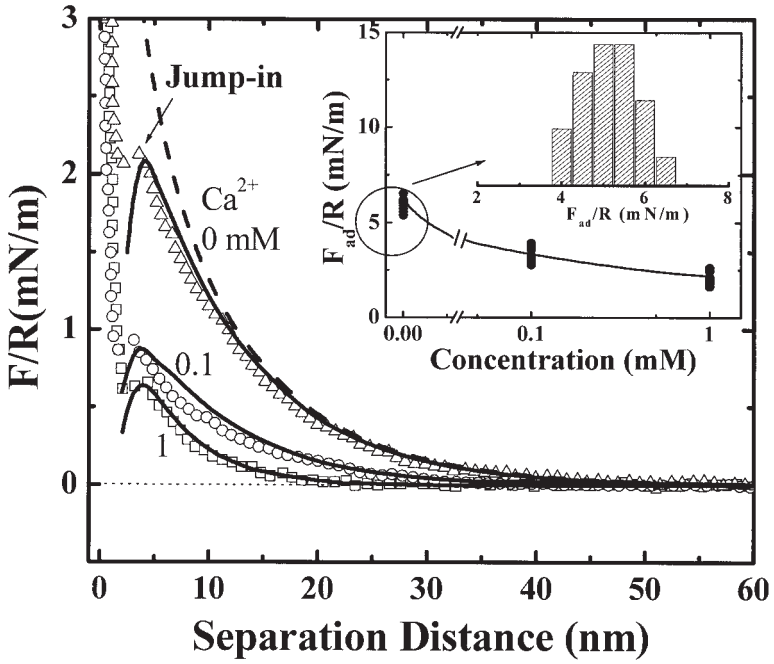

Figure 8. Normalized interaction forces (F/R) between bitumen surfaces as a function of separation distance at pH 8.2 in 1 mM KCl solutions containing different concentration of calcium ions.

Solid lines represent the extended DLVO fitting using $A_{BWB} = 2.8 \times 10^{-21}$ J with the best-fitted decay length, Stern potential and hydrophobic force constant being: 0 mM Ca^{2+} (up triangles): $\kappa^{-1} = 9.4$ nm, $\psi_B = -74$ mV, $K = 10 \times 10^{-20}$ J; 0.1 mM Ca^{2+} (circles): $\kappa^{-1} = 8.3$ nm, $\psi_B = -41$ mV, $K = 6 \times 10^{-20}$ J; 1 mM Ca^{2+} (squares): $\kappa^{-1} = 4.8$ nm, $\psi_B = -31$ mV, $K = 3.5 \times 10^{-20}$ J. The dashed line represents the DLVO fitting using $A_{131} = 2.8 \times 10^{-21}$ J with a best-fitted decay length, Stern potential being: 0 mM Ca^{2+} (up triangles): $\kappa^{-1} = 9.4$ nm, $\psi_B = -74$ mV. Insert: normalized adhesive forces (F_{ad}/R) measured at loading forces of 8–10 mN/m as a function of calcium concentration. Inner insert: distribution of normalized adhesive forces (F_{ad}/R) in a 1 mM KCl solution at pH 8.2.

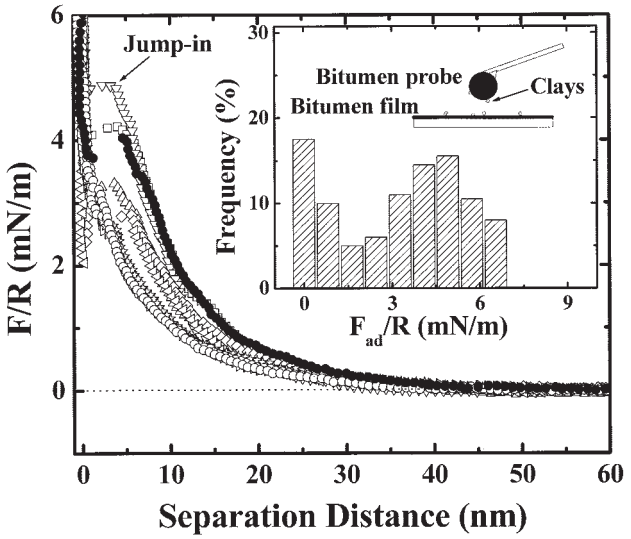

Figure 9. Normalized interaction forces (*F*/*R*) between bitumen surfaces as a function of separation distance at pH 8.2 in solutions containing 1 mM KCl.

The surfaces were conditioned before AFM force measurement with a 0.1% montmorillonite suspension containing 1 mM KCl. Insert: distribution of normalized adhesive forces (F_{ad}/R) measured at loading forces of 8–10 mN/m.

ments by Kasongo et al. (2000) and Liu et al. (2002a) showed that the contact angle of an air bubble on a bitumen surface immersed in water was about 70°. With such hydrophobic bitumen surface, the presence of hydrophobic force between two bitumen surfaces is not unexpected. The fitted parameter *K*, describing the strength of the hydrophobic force, decreased from 10×10^{-20} J for the case of no calcium addition to 3.5×10^{-20} J with 1 mM calcium addition. This indicates that the attractive hydrophobic force between bitumen and bitumen becomes weaker in the presence of calcium ions. The adhesion forces between bitumen and bitumen were also decreased from 5.8 to 2 mN/m upon the addition of 1 mM calcium, as shown by the insert of Figure 8. The results suggest that calcium adsorption on the bitumen surface decreases the surface hydrophobicity of the bitumen and the adhesion forces between two bitumen surfaces. Clearly, the presence of calcium ions in the industrial process water as used in the oil sands extraction is undesirable for agglomeration and coalescence of bitumen droplets.

Presence of Montmorillonite Clay without Calcium. After the bitumen surface was conditioned with a 0.1% fine montmorillonite clay suspension containing 1 mM KCl in the absence of calcium ions, the colloidal surface force measurements were conducted and the results are shown in Figure 9. The results show that the repulsive forces between two bitumen surfaces were substantially increased, which cannot be described with the classical or extended DLVO theory. To account for the very strong repulsive forces, one needs to assume some coverage on the bitumen surface by fine montmorillonite clay particles. It is interesting to note that, in some cases, a noticeable "jump-in" was observed after encountering a strong repulsive barrier at a separation distance of 4–7 nm, shown by the arrow in Figure 9. The observed sudden "jump-in" after encountering a strong repulsive barrier cannot be explained by either van der Waals or hydrophobic forces. A possible explanation is that in the absence of calcium ions the montmorillonite clay particles deposit weakly and sparsely on the bitumen surface. This is plausible because only the amphoteric edge of layer-structured clay particles is amenable for deposition on the negatively charged bitumen surface and the edge accounts for only 1% of total surface area of particles (Sondi et al., 1996, 1997). As schematically illustrated in Figure 10, the weakly and sparsely bound clay particles on bitumen surfaces were pushed laterally under a threshold force applied by the AFM cantilever when the two surfaces were brought close to each other.

A similar observation was reported when forces were measured between an AFM tip and a mica surface bearing adsorbed aggregates of dodecyltrimethylammonium bromide (DTAB) (Ducker and Wanless, 1996). The observed "jump-in" after encountering a strong repulsive force was attributed to the "squeezing out" of the surfactant aggregates. The presence of montmorillonite clay particles on the bitumen surface can be further inferred from the distribution nature of the measured adhesion forces. Compared with the adhesion forces measured with bitumen surfaces without conditioning with clay suspensions, as is shown in the inner inset of Figure 8, these adhesion forces are much more widely distributed, as shown in the insert of Figure 9. The adhesion forces between two bitumen surfaces conditioned with clay suspensions were mostly distributed in the range of 4–7 mN/m and in a number of cases reduced to zero, which can possibly be attributed to no clays and to some clays on the bitumen surface, respectively. This finding further confirms the weak and sparse deposition of montmorillonite particles on the bitumen surface. In all, the results of force profiles clearly indicate that conditioning the bitumen surfaces with 0.1% montmorillonite clay suspension can to some extent increase the repulsive force and diminish the adhesion force between two bitumen surfaces. This confirms the weak attachment of montmorillonite clay particles on a bitumen surface, as interpreted from the force profiles shown in Figures 4 and 5.

Presence of Montmorillonite Clay with Calcium Addition. When bitumen surfaces are conditioned with 0.1% montmorillonite clay suspensions containing 1 mM KCl and 1 mM calcium ions, the force profiles between the bitumen surfaces become monotonically repulsive without a "jump-in," as shown in Figure 11. The range of the repulsion is reduced substantially over a separation range of 5–20 nm. The force

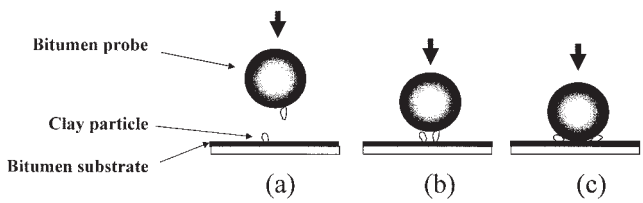

Figure 10. Possible interactions between bitumen surfaces after conditioning with a 0.1% montmorillonite suspension containing 1 mM KCl solution at pH 8.2 in AFM.

(a) Approaching with sparse montmorillonite particles attached weakly on the bitumen surface; (b) initial contact; (c) "jump-in" when "squeezing-out" of montmorillonite particle under threshold forces.

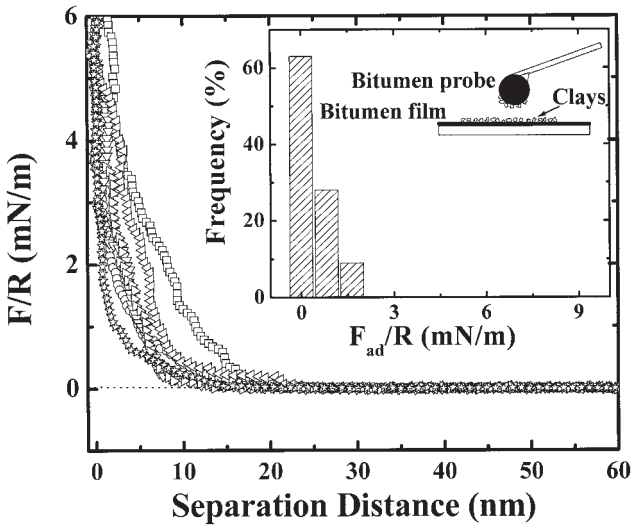

Figure 11. Normalized interaction forces (*F*/*R*) between bitumen surfaces as a function of separation distance at pH 8.2 in a solution containing 1 mM KCl and 1 mM Ca^{2+}.

The surfaces were conditioned before AFM force measurement with a 0.1% montmorillonite suspension containing 1 mM KCl and 1 mM Ca^{2+}. Insert: distribution of normalized adhesive forces (F_{ad}/R) measured at loading forces of 8–10 mN/m.

profiles cannot be fitted with the classical or extended DLVO theory. In this case, the adhesion forces were reduced significantly, in some cases to zero, as shown in the insert of Figure 11. Compared with Figures 8 and 9, the absence of "jump-in" in the force profiles of Figure 11 and reduction in the adhesion forces imply that a strong and dense deposition of montmorillonite clay particles occurs on the bitumen surface in the presence of 1 mM calcium ions, as depicted in the insert of Figure 11. This is quite plausible because both the edge and basal plane of montmorillonite particles can attach to the bitumen surface with calcium ion as a bridge. In this case, the attached clay particles can no longer be squeezed out. As a result, the bitumen surface bearing densely montmorillonite particles becomes clay-like. The interpretation mentioned above is consistent with the measured strong adhesion forces and the much suppressed long-range repulsive forces between bitumen and montmorillonite clay particles in 1 mM calcium solutions (Figures 4 and 5). With respect to the bitumen extraction, any presence of montmorillonite clays on bitumen surfaces in the presence of 1 mM calcium would set up an obstacle for bitumen droplets to coagulate with each other and to attach to air bubbles, thereby contributing to a poor bitumen recovery.

Zeta potential distribution measurement

To further confirm slime-coating of montmorillonite, and not kaolinite clay, on bitumen surfaces in the presence of 1 mM calcium ions, as interpreted from the measured force profiles, the zeta potential distributions of bitumen droplets and clay particles, individually and in a mixture, were measured in the presence of 1 mM calcium ions. As shown in Figure 12a, the zeta potential distributions of bitumen and montmorillonite clay suspension, measured individually, were centered at −38 and −11 mV, respectively. As shown in Figure 12b, for a mixture of bitumen and montmorillonite clays, only one distribution peak centered at −12 mV was observed. This value corresponds closely to the value for montmorillonite clay suspension alone (−11 mV). The absence of the zeta potential distribution peak measured with bitumen emulsion alone suggests that the bitumen droplets were fully covered by montmorillonite clay particles. The zeta potential distribution measurements confirm that there is a strong attachment between the bitumen and montmorillonite clays, as would be anticipated for a system having a weak repulsive force with a strong adhesion (see Figures 4b and 5b).

For the system of bitumen–kaolinite clay, the zeta potential distributions of bitumen and kaolinite measured individually are shown in Figure 12c. Two distinct peaks centered at −38 and −9 mV for bitumen and kaolinite were observed, respectively. However, a similar zeta potential distribution histogram was obtained for a mixture of bitumen and kaolinite, as shown

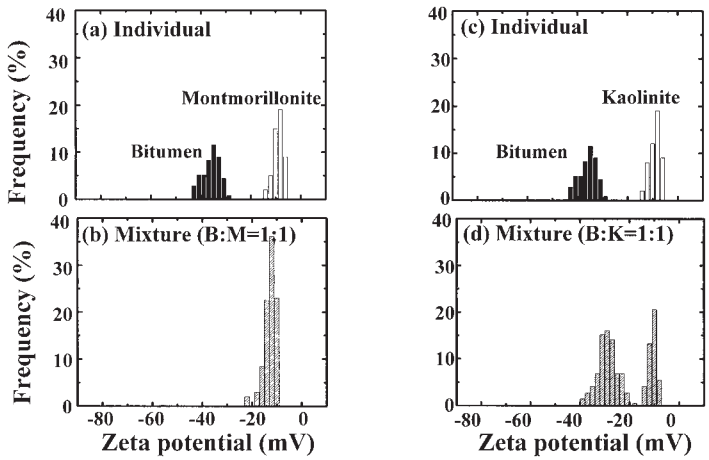

Figure 12. Zeta potential distributions for individual bitumen droplets and clay particles, and their mixture in 1 mM KCl solution containing 1 mM Ca^{2+} at pH 8.2.

(a) and (b): Bitumen–montmorillonite; (c) and (d): bitumen–kaolinite.

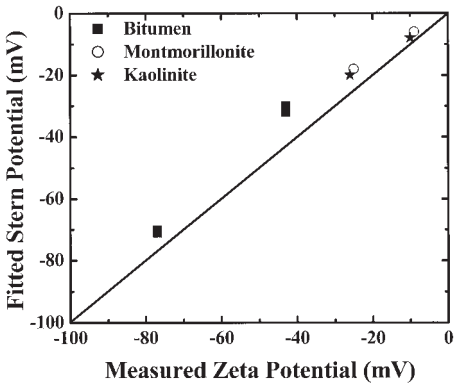

Figure 13. Comparison of the best-fitted Stern potentials derived from the measured force profiles with the classical or extended DLVO theory and the measured corresponding zeta potentials.

Bitumen droplets (square symbols), montmorillonite (circle symbols), and kaolinite (star symbols).

in Figure 12d. This observation implies that bitumen and kaolinite are very weakly coagulated, which is consistent with the interpretation from the measured adhesion force (see Figure 7b).

General remarks

Although the force–distance data obtained from the surface force measurements show scatter, the trends are clear and they shed light on a complex industrial system. The measured force profiles were fitted by the classical and extended DLVO theory with constant surface charge density for bitumen and constant surface potential for clays as boundary conditions. As shown by solid lines in Figures 4, 6, and 8, measurements at a separation distance of greater than 5–8 nm for a large number of bitumen–clay pairs and bitumen–bitumen pairs, without conditioning with montmorillonite clay suspensions, can be predicted with the classical and extended DLVO theory within the scatter range. The fitted Debye decay lengths (κ^{-1}) agree well with those calculated for the electrolyte concentrations as used in the experiments. Furthermore, the fitted Stern potentials are slightly smaller than the measured zeta potentials, as shown in Figure 13. Considering the roughness of the clays used in the force measurement, this level of discrepancy is expected. It is important to note that similar fittings with a boundary condition of constant surface charge density for both surfaces result in fitted Stern potentials much smaller than the measured zeta potentials.

The microscale colloidal force measurement using AFM provided insights into megascale industrial operations of oil sands extraction. The strong slime coating of montmorillonite clays on the bitumen surface in the presence of 1 mM calcium is a good candidate as being the main cause for depressed bitumen recovery of poor processing ores containing high fines and divalent cations. It is anticipated that any changes that cause an increase in the electrostatic repulsion between bitumen and montmorillonite clays or fines by a dispersant addition, such as sodium silicates or phosphates, would mitigate the depression of bitumen recovery by flotation.

Conclusions

(1) Montmorillonite clays possess some unique surface properties: a large capacity for adsorption of calcium ions and pH-independent zeta potentials. Kaolinite behaves as a typical mineral.

(2) In the absence of calcium, montmorillonite clays weakly attach on the bitumen surface. With the addition of 1 mM calcium, montmorillonite clay attaches strongly to the bitumen surface. The depressed electrostatic double-layer forces and increased adhesive forces between bitumen and montmorillonite clays are responsible for the observed strong attachment, thereby presenting a barrier for bitumen–air attachment and bitumen–bitumen coagulation, leading to poor bitumen recovery.

(3) Kaolinite clays can only weakly attach to the bitumen surface in the absence or presence of calcium ions. Although the electrostatic double-layer forces were suppressed with the addition of 1 mM calcium, the weak adhesive forces between the two surfaces are responsible for weak kaolinite attachment to the bitumen.

(4) The measured force profiles can be satisfactorily used to qualitatively interpret the role of fine clays in bitumen extraction from oil sands, which was demonstrated with zeta potential distribution measurements. The low bitumen recovery of poor processing ores with a high fine content and a high divalent cation concentration in the process water can be understood with microscale colloidal force measurements using AFM.

Acknowledgments

The authors acknowledge the financial support from COURSE (Coordination of University Research for Synergy and Effectiveness), with Syncrude Canada Ltd. and Albian Sands Inc. as industrial partners; Natural Sciences and Engineering Research Council of Canada (NSERC); and NSERC Chair in Oil Sands Engineering. The provision of oil sand samples by Syncrude Canada Ltd. is also acknowledged.

Literature Cited

Ducker, W. A., T. J. Senden, and R. M. Pashley, "Measurement of Forces in Liquids Using a Force Microscope," *Langmuir*, **8**(7), 1831 (1992).

Ducker, W. A., and E. J. Wanless, "Surface-Aggregate Shape Transformation," *Langmuir*, **12**(24), 5915 (1996).

Duran, J. D. G., M. M. Ramos-Tejada, F. J. Arroyo, and F. Gonzalez-Caballero, "Rheological and Electrokinetic Properties of Sodium Montmorillonite Suspensions: I. Rheological Properties and Interparticle Energy of Interaction," *J. Colloid Interface Sci.*, **229**(1), 107 (2000).

Fuerstenau, D. W., "Fine Particle Flotation," *Fine Particle Processing*, Somasundaran, P., ed., The Society of AIME, New York, pp. 669–705 (1980).

Gu, G., Z. Xu, K. Nandakumar, and J. H. Masliyah, "Effects of Physical Environment on Induction Time of Air–Bitumen Attachment," *Int. J. Miner. Process.*, **69**, 235 (2003).

Heath, D., and T. F. Tadros, "Influence of pH, Electrolyte, and Polyvinyl-Alcohol addition on the Rheological Characteristics of Aqueous Dispersions of Sodium Montmorillonite," *J. Colloid Interface Sci.*, **93**(2), 307 (1983).

Hepler, L. G., and C. Hsi, "AOSTRA Technical Handbook on Oil Sands, Bitumen and Heavy Oils," AOSTRA Technical Publication Series #6, Alberta Oil Sands Technology and Research Authority, Edmonton, AB, Canada (1989).

Hepler, L. G., and R. G. Smith, "The Alberta Oil Sands: Industrial Procedures for Extraction and Some Recent Fundamental Research," AOSTRA Technical Publication Series #14, Alberta Oil Sands Technology and Research Authority, Edmonton, AB, Canada (1994).

Hunter, J. R., *Introduction to Modern Colloid Science*, Oxford Univ. Press, New York (1993).
Israelachvili, J. N., *Intermolecular and Surface Forces*, 2nd Edition, Academic Press, San Diego, CA (1991).
Kappl, M., and H. J. Butt, "The Colloidal Probe Technique and Its Application to Adhesion Force Measurements," *Part. Part. Syst. Char.*, **19**(3), 129 (2002).
Kasongo, T., Z. Zhou, Z. Xu, and J. H. Masliyah, "Effect of Clays and Calcium Ions on Bitumen Extraction from Athabasca Oil Sands Using Flotation," *Can. J. Chem. Eng.*, **78**(4), 674 (2000).
Liu, J., "Role of Colloidal Interactions between Oil Sand Components in Bitumen Recovery from Oil Sands," PhD Thesis, University of Alberta, Canada (2004).
Liu, J., Z. Xu, and J. H. Masliyah, "Studies on Bitumen–Silica Interaction in Aqueous Solutions by Atomic Force Microscopy," *Langmuir*, **19**(9), 3911 (2003).
Liu, J., Z. Zhou, and Z. Xu, "Electrokinetic Study of Hexane Droplets in Surfactant Solutions and Process Water of Bitumen Extraction Systems," *Ind. Eng. Chem. Res.*, **41**(1), 52 (2002b).
Liu, J., Z. Zhou, Z. Xu, and J. H. Masliyah, "Interactions between Clays and Bitumen in Aqueous Media from the Measurement of Zeta Potential Distributions," *J. Colloid Interface Sci.*, **252**(2), 409 (2002a).
Liu, J., Z. Zhou, Z. Xu, J. Masliyah, J. Choung, and T. Kasongo, "Study of Slime Coatings in Flotation by Electrophoretic Mobility Distribution Measurement," Proc. of 34th Canadian Mineral Processing Operators Conference, J. Nesset, ed., CIM, Ottawa, Canada, 403–416 (2002c).
Masliyah, J. H., "Electrokinetic Transport Phenomena," AOSTRA Series 12, University of Alberta, Edmonton, AB, Canada (1994).
Olphen, H. V., *An Introduction to Clay Colloid Chemistry*, 2nd Edition, Wiley, New York (1976).
Rabinovich, Y. I., and R. H. Yoon, "Use of Atomic Force Microscope for the Measurements of Hydrophobic Forces between Silanated Silica Plate and Glass Sphere," *Langmuir*, **10**(6), 1903 (1994).
Sanford, E. C., "Processibility of Athabasca Oil Sand: Inter-relationship Between Oil and Fine Sands," *Can. J. Chem. Eng.*, **61**(4), 554 (1983).
Sanford, E. C., and F. A. Seyer, "Processibility of Athabasca Tar Sand Using Batch Extraction Unit: The Role of NaOH," *CIM Bull.*, **72**, 164 (1979).
Sivamohan, R., "The Problem of Recovering Very Fine Particles in Mineral Processing—A Review," *Int. J. Miner. Process*, **28**, 247 (1990).
Smith, R. G., and L. L. Schramm, " The Influence of Mineral Components on the Generation of Natural Surfactants From Athabasca Oil Sands in the Alkaline Hot Water Process," *Fuel Process. Technol.*, **30**(1), 1 (1992).
Sondi, I., J. Biscan, and V. Pravdic, "Electrokinetics of Pure Clay Minerals Revisited," *J. Colloid Interface Sci.*, **178**(2), 514 (1996).
Sondi, I., O. Milat, and V. Pravdic, "Electrokinetic Potentials of Clay Surfaces Modified by Polymers," *J. Colloid Interface Sci.*, **189**(1), 66 (1997).
Takamura, K., and D. Wallace, "The Physical Chemistry of the Hot Water Process," *J. Can. Petrol. Technol.* **27**, 98 (1988).
Veeramasuneni, S., M. R. Yalamanchili, and J. D. Miller, "Measurement of Interaction Force between Silica and Alumina by Atomic Force Microscope," *J. Colloid Interface Sci.*, **184**(2), 594 (1996).
Vincent, B., "The van der Waals Attraction between Colloidal Particles Having Adsorbed Layers: II. Calculation of Interaction Curves," *J. Colloid Interface Sci.*, **42**(2), 270 (1973).
Warszynski, P., and Z. Adamczyk, "Calculation of Double Layer Electrostatic Interaction for the Sphere/Plane Geometry," *J. Colloid Interface Sci.*, **187**, 283 (1997).
Xu, Z., J. Liu, J. Choung, and Z. Zhou, "Electrokinetic Study of Clay Interactions with Coal in Flotation," *Int. J. Miner. Proc.*, **68**, 183 (2003).
Yang, C., "Attachment of Fine Gas Bubbles onto a Solid Surface and Eelectrokinetics of Gas Bubbles," PhD Thesis, University of Alberta, Canada (2000a).
Yang, C., T. Dabros, D. Q. Li, J. Czarnecki, and J. H. Masliyah, "Visualizing Method for Study of Micron Bubble Attachment onto a Solid Surface under Varying Physicochemical Conditions," *Ind. Eng. Chem. Res.*, **39**(12), 4949 (2000b).
Zhou, Z. A., Z. Xu, J. H. Masliyah, and J. Czarnecki, "Coagulation of Bitumen with Fine Silica in Model Systems," *Colloids Surf. A*, **148**(3), 199 (1999).

Manuscript received Jul. 23, 2003, and revision received Dec. 22, 2003.